A Germination model for *Alexandrium fundyense*

Updated August 14, 2006

Charles Stock

Introduction

This document gives a detailed description of the *Alexandrium fundyense* germination model that was developed as part of the ECOHAB-Gulf of Maine program. A reference for the material described herein is provided by Anderson et al. (2005), and versions of this model have been used in several other studies (Mcgillicuddy et al. 2003; McGillicuddy et al. 2005; Stock et al. 2005). A model timeline, which summarizes adjustments, updates, and corrections can be found at:

http://www.whoi.edu/science/cohh/alexbiomodels.htm

This document describes the germination component of version 3.1 of the *A. fundyense* biological model. This is the model described in Anderson et al. (2005), with a few minor corrections to figures (see captions of Fig. 8 and Fig. 12).

Briefly, the modeled rate of germination (G, % of initial cysts/day) is a function of bottom water temperature (T, ^{o}C), the day-light averaged irradiance (E, watts/m^2, 8 AM-6 PM), and an endogenous clock ($EC(t)$, where t is the year-day):

$$G(T,E,t) = EC(t) \times G(T,E)$$

The flux of *A. fundyense* from the cyst bed to the water column (F_g) is then estimated by applying the germination rate to an observed cyst distribution:

$$\mathrm{F_g} = \int_0^{d_g} \left(G(T,E(z),t) \times [Cysts/cm^3]_o \right) dz$$

where d_g, the "germination depth" in centimeters, is an estimate of the depth of sediment over which cysts are exposed to oxygen and can gain access to the water column through the sediment grain matrix. It is notable that the germination rate multiplies the initial cyst concentration: $[Cysts/cm^3]_o$, rather then the present level of cysts. This is done for consistency with the germination time series data (see below). The remainder of this document describes the three primary parts of the germination model in detail:

- The temperature and light dependence
- The endogenous clock
- The germination depth estimation

Each section begins by describing the data and/or studies from which the function is formed. The function construction is then presented in detail, followed by a brief discussion of assumptions and limitations.

1 The Temperature and Light Dependence

1.1 Background and Data

Laboratory data from two cyst isolates was used to construct the dependence of *A. fundyense* germination on temperature and light. The first isolate was collected offshore of Casco Bay Maine (station 38, Latitude 43° 30.29'N; Longitude 69° 52.72'W) in approximately 125 meters of water. The second isolate was taken near the mouth of the Bay of Fundy (station 4, Latitude 44° 53.47'N, Longitude 66° 48.86'W) in 135-140 meters of water (Figure 1). Time series of germination were tracked with cysts exposed to water temperatures of 2, 4, 6, 8, and 15 °C in "light" and "dark" conditions. The

"light" condition was classified as an irradiance of 5-15 μE/(m^2 s) applied on a 14:10 LD cycle. The "dark" condition excluded all light.

The experimental methods are described in detail in Anderson et al. (2005). Briefly, cysts were collected from the top 2-6 cm of sediment and stored under anoxic conditions until 90-93% germination potential was shown (i.e. it was ensured that the germination rate would reflect the rate obtainable when the endogenous clock was not limiting). The sediment sample was then combined with F/2 media, made into uniform slurry, and divided into separate flasks for incubation under the various experimental conditions. The flasks were then harvested over time to produce germination and fluorescence time series for each condition (Figure 2).

1.2 Function Construction

The slope of a linear fit was used to estimate a germination rate for each experimental time series. The fitting procedure was complicated by the asymptotic behavior of the data points as the germination potential was approached. To capture the slope of the germination curve over the time during which the majority of cysts germinate, only points of ≤ 90% germination and those taken ≤ 75 days after the beginning of the time series are included in the fit. The fitted lines were not forced through the origin to minimize the influence of any necessary acclimation to experimental conditions after transfer from cold, dark storage. The resulting slopes fit are shown in Figures 3-6 and summarized in Table 1.

The discrete germination rates in Table 1 were interpolated and extrapolated to other temperatures by fitting to the function:

$$G(T, E_{\lg t}) = G_{\min}(E_{\lg t}) + \frac{(G_{\max}(E_{\lg t}) - G_{\min}(E_{\lg t}))}{2} \times \{\tanh(\alpha(E_{\lg t})T - \beta(E_{\lg t})) + 1\}$$

$$G(T, E_{drk}) = G_{\min}(E_{drk}) + \frac{(G_{\max}(E_{drk}) - G_{\min}(E_{drk}))}{2} \times \{\tanh(\alpha(E_{drk})T - \beta(E_{drk})) + 1\}$$

Where E_{lgt} and E_{drk} refer to the irradiance under the "light" and "dark" experimental conditions. The hyperbolic tangent function allows for a linear relationship over moderate temperatures (slope = α) that is consistent with many previous investigations of seed germination behavior (Bewley and Black 1978). It also allows for maximum germination rates ($G_{\max}$) and minimum germination rates ($G_{\min}$) to occur over broad ranges, which is suggested by previous observations of *A. fundyense* germination behavior (Anderson 1998). Fitted parameters are given in Table 2 and the resulting function is shown in Figure 7.

The light response is interpolated and extrapolated to other values using:

$$G(T, E) = G(T, E_{\lg t}) \qquad E \geq E_{\lg t}$$

$$G(T, E) = G(T, E_{drk}) \qquad E \leq E_{drk}$$

$$G(T, E) = G(T, E_{drk}) + (G(T, E_{\lg t}) - G(T, E_{drk})) \times \frac{E - E_{drk}}{E_{\lg t} - E_{drk}} \qquad E_{\lg t} > E > E_{drk}$$

For the purpose of this calculation, E_{drk} is taken to be 1% of E_{lgt}. The irradiance used is the average value over 14 daylight hours (e.g. 6 AM - 8 PM), as experimental light conditions were on a 14:10 cycle. To approximate the light reaching the cysts within the sediment, observed surface shortwave irradiance is exponentially attenuated in the water column (k_w) and within the sediment (k_s). The resulting function is shown in Figure 8. It is notable that the germination rate multiplies the initial cyst concentration, and not the

concentration at any given time. This is done to be consistent with the germination time series data.

1.3 Discussion

The curve fitting thresholds and methods were chosen because 1) they are generally effective at minimizing contamination of the slope estimates by the asymptotic behavior of the germination time series as the germination potential is approached, 2) they did not lead to the elimination of large numbers of data points from consideration. Other thresholds were evaluated and performed fairly well, but those chosen exhibited the most robust performance over the range of experimental conditions. There are some cases (e.g. 6^{o} for WGOM isolates in the light) where subjective fitting may shift the result slightly. However, given the level of noise in the data and the uncertainty in the resulting slopes, it would tenuous to make any substantial inference based on the small changes that such subjective adjustments would create.

Consideration was also given to the usage of more complex functional forms for the fitting. However, such efforts are restricted by the necessity of associating one representative rate with each experimental condition. In addition, the increasing portions of the curves generally show a high degree of linearity and increasing complexity in the functional form is likely to make little difference to the overall character of the germination rate function.

The functions require a large amount of extrapolation and interpolation. Sensitivity tests within the Gulf of Maine (Stock et al. 2005) suggest that the uncertainty produced by the details of this interpolation and extrapolation is small relative to the

uncertainty contributed by other aspects of the germination and growth model. However, this sensitivity is dependent upon the setting in which the model is used and should be revisited if the model is being applied in a markedly different environment (e.g. a shallow enclosed salt pond).

The strongest suggestion that differences may exist between the two isolates comes from the 8°C time series in the dark condition. In the other 7 cases where comparison between the WGOM isolate and the EGOM isolate is possible, estimated rates are very similar. Thus, despite the discrepancy at 8°C in the dark, differences are minimal and no attempt was made to construct separate functions for each strain.

2. The Endogenous Clock

2.1 Background and Data

The germination potential of *A. fundyense* is modulated by an internal endogenous clock (Anderson and Keafer 1987; Matrai et al. 2005). This clock is capable of preventing germination even when environmental conditions are favorable. Experimental data for construction of the endogenous clock were drawn from experiments by Anderson and Keafer (Figure 9), Matrai et al. (Figure 10) and from data presented by Bronzino (1998), (Figure 11). The isolates used for the three data sets are summarized in Table 3.

The experimental protocol was similar in all cases. Detailed descriptions appear in Matrai et al. (2005) and Bronzino et al. (1998). Briefly, once sediment samples were collected they, along with the cysts within them, were stored in dark, cold (2° C), anoxic conditions. Periodically (every 2 weeks in the Bronzino et al. and Matrai et al. experiments, and slightly less often in the earlier data) 30 cysts were isolated from the

stored sediment and transferred to a culture well with f/2 medium. These wells were placed in an incubator at 15^{o} C and subject to a 14:10 light/dark cycle with greater than 150 $\mu E/(m^2 s)$ of light. The germination of cysts in the 30 well plates was tracked periodically. Matrai et al. report the percentage of cysts germinated after 6 weeks, Bronzino and Anderson and Keafer report values after 4 weeks. There were other small differences in experimental technique between the different data sets. During the isolations in the 1980's, sediment was stored as a bulk sample, which required that storage conditions be compromised for short periods during the isolation process. Thereafter, the sediment for each isolation was stored in separate vials. Also, Matrai et al. (2005) took slightly more exhaustive measures to ensure anoxic conditions during storage. However, in all cases, cysts taken out of storage showed a lack of fluorescence suggesting that contamination with oxygen during storage was minimal and probably did not influence results (Keafer, personal communication).

Despite the similarities in experimental conditions, the different isolates show considerable variability in both the timing and the duration of peaks in germination potential. In the station 29 data, the three isolates show an initial peak in germination potential at three different times. Cysts from the 1984 sample reach maximum germination potential in early March, while the 1985 sample and 1987 samples reach germination peaks in the late spring and early summer. The 1985 sample also shows a more gradual climb to peak conditions than many of the other cyst samples. The results of Matrai et al. show an initial peak in germination potential for experiments initiated in February and March, and in this way are consistent with the initial peak of the 1984 station 29 cysts. Station 94 shows a more elongated decline from the peak than the

station 61 and station 4 cysts. Lastly, the station 38 data show a late March/early April initial peak, and a slow decline in germination potential that is even more pronounced then station 94.

Potential reasons for the different patterns exhibited in Figures 9-11 are discussed in Anderson (1998) and by Matrai et al (2005). One possibility mentioned is that cysts within a particular sediment sample contain a mixture of strains with different genotypes, each with somewhat different endogenous clock strategies. If this were the case, one would expect variability based on the relative proportion of the different genotypes during any given year or at a particular location. A second possibility is that the different patterns result from interaction with environmental cues that "entrain" the endogenous clock in an external rhythm. This process is well described in Sweeney (1969):

> Just as in physical oscillations, the frequency of rhythms may be forced to match exactly that of some external oscillation, the alternation of light and darkness for example. When this occurs, the rhythm is said to be entrained by the external oscillation. The signal responsible for the entrainment has been called the 'zeitgeber' or 'time-giver'. Entrainment, of course, can only take place while the external oscillation is actually present. When a rhythm is not entrained, it is said to be free running and now shows its natural period.

Matrai et al. (2005) estimated a natural period of 11 months (+/- 2 months). However, the predictable seasonal timing of *A. fundyense* blooms suggests that they have become entrained by a 12-month environmental rhythm. This entrainment phenomenon links the properties of clock to external cues: Although the clock operates in the absence of any environmental cues, environmental cues can influence the properties of the clock. This

makes the task of constructing a function based on the data in Figures 9-11 (i.e. constant environmental conditions) for use in the model (variable environmental conditions) more difficult. The validity of any representative endogenous clock constructed from the laboratory data described above requires assumptions about the relationship between the free-running and entrained rhythms that will be discussed below.

2.2 Function Construction

Data used to construct a representative endogenous clock cycle were restricted to those that 1) were taken during the first year after the cyst isolation date, and 2) were taken before the second observed rise in the germination potential (filled dots in figures 9-11). These points were binned into months according to the mid-point of the 4 or 6 week experiment. The median value of the experimental points in each bin was then used to assign a representative germination potential for each bin. The resulting function is shown in Figure 12 and the values for each month are reported in Table 4. The germination potential for each month is normalized with the maximum germination potential to form the normalized germination potential (NGP, Table 4). The multiplier $EC(t)$ within the germination model cycles between values of the NGP for each month using a linear interpolation.

Only data from the first 12 months after isolation were used because this minimizes shifts in the phase at a given yearday resulting from transition back to the natural period of the clock (~11 months) once constant environmental conditions are established. Peaks in the laboratory measured germination potential will be observed approximately 1 month earlier for each year that the cells have been isolated from environmental cues. If these additional years were included, there would be a bias

toward earlier germination peaks in the representative model clock relative to the entrained clock (which the model hopes to approximate). The additional condition eliminating points associated with the second observed rise in the germination potential was added as an additional safeguard against this kind of contamination.

Experimental points are shifted to the mid-point of the experimental period because the reported germination potential represents an integration of the germination potential over the 4 (or 6) week experimental period. This is likely to have variable effects depending on the rate of change of the germination potential over the time of the experiment, the direction of that change, and the rate of germination. For example, if the rate of germination was fast relative to the experimental period and the germination potential was increasing, the potential recorded would reflect the potential at the end of the experimental period. If the germination potential was decreasing and the rate of germination was still fast, the opposite would be true. That is, cysts would quickly germinate at the beginning of the experimental period (when the germination potential was high), and the decreasing potential later during the period would have little effect. Given that germination rates under the conditions used for the endogenous clock experiment (~5-10 %/day) act on time scales similar to the experimental period, the simplest way to minimize uncertainty associated with the temporal placement of the measured germination potential is to center it within the time period covered by the experiment.

The use of the median is designed to prevent the creation of a representative cycle that, because of averaging in variable areas, has properties that are dissimilar from any of the data sets contributing to it. Most notably, use of the mean would lead to a greatly

damped oscillation. The peak germination potential would only be ~ 85%, while the minimum would be ~30%. The median focuses the fit on characteristics common to the majority of the cycles: A sharp late fall/winter low in the germination potential followed by an abrupt spring rise to just under 100%, then maintenance of the high potential throughout the spring and majority of the summer until a more gradual late summer, early fall decline.

2.3 Discussion

The ability to construct a representative endogenous clock function for *A. fundyense* in the Gulf of Maine based on the laboratory data described above rests on two primary assumptions:

1. The phase of the clock does not change when cysts are removed from the sediment and stored.
2. The first-order characteristics of the free-running clock (i.e. the duration and size of the peaks and troughs) are similar to those of the entrained clock.

Some support for these assertions is provided by measurement of cyst fluorescence in sediments from the field (Anderson and Keafer 1985; Anderson et al. 2005). Additional support is sparse. However, the assumption that the free-running clock is not drastically different than the characteristics favored by the environmental patterns that the clock has evolved to function within seems a reasonable starting point.

The influence imposed upon the endogenous clock by environmental cues means that care should be taken when applying this function to regions where the seasonal cycle is shifted significantly relative to that of the Gulf of Maine. Even when environmental

conditions are similar, the variability between isolates suggest considerable uncertainty in the details of the function and care should be taken to avoid overly fine inferences regarding the temporal properties of the source as they relate to the endogenous clock.

3. Influence of Sediment Mixing

3.1 Background and Data

A. fundyense cysts reside in a dynamic sediment environment whose physical, chemical, and biological properties can have a profound influence on germination. Cysts can remain viable within the sediment for years and cyst distributions within the sediment show considerable vertical structure related to past history of deposition, germination, and sediment mixing dynamics (Anderson et al. 1982; Keafer et al. 1992). Sediment dynamics can influence the cyst source in ways not within the basic model described above. Additional light attenuation within the sediment can slow rates below those shown in Figure 8, oxygen depletion near the surface of the sediment can severely limit the depth over which cysts can germinate (Anderson et al. 1987), and the impairment of upward vegetative cell movement within the sediment grain matrix can prevent newly germinated cells from ever reaching the water column. Each of these factors will be discussed briefly below after which the current modeling approach will be described and discussed.

Light attenuation within the sediment can be substantial. Kuhl and Jorgensen (1994) report a range of wavelength dependent diffuse light attenuation rates in sandy coastal sediments (63-250 μM grain size with diatom detritus) from 2-5 mm^{-1}, roughly ten thousand times the attenuation rate in the water column in typical coastal areas. It is

thus necessary to consider light attenuation within the sediment for cysts lying even 1 mm below the sediment surface, as this is equivalent to as much as 25m of water column in typical coastal waters (~0.2 m^{-1}).

Anaerobic conditions completely suppress the germination of *A. fundyense* as well as the fluorescence that comes before it (Anderson et al. 1987). Depletion of oxygen in the surface sediments is dependent upon multiple physical and biological factors including the amount of oxygen in bottom waters, mixing within the sediment, and the flux of organic matter to the sediment. In the Gulf of Maine, Anderson and Keafer (1985) noted that fluorescence of cysts was very low (7% on average) within the 1-2 cm sediment depth interval at station 29. Cysts taken above 1 cm showed a considerable increase (39% on average, with a peak of 83% during the late spring). Results from a second nearby station (61 meters depth) are similar, although fluorescence at both depths was lower than those at the respective depths for station 29 (10% and 1% respectively, with a high value in the 0-1 cm interval of 23%). In addition, Hines (1991) noted anaerobic metabolisms were prevalent 1 cm into the water column for 2 of 3 cores in the western Gulf of Maine. The third core showed slowed rates of anaerobic activity at 1 cm and much increased rates at 3 cm.

The role of the sediment as a potential barrier between recently germinated cells and the water column can be stated in geometrical terms. The resting cyst and the vegetative cells produced upon germination are approximately 50 μM in diameter. Thus, a cyst germinating at 1 cm is likely to be nearly 200 body lengths away from the sediment surface. Presumably, this distance is blocked by a matrix of gravel, sand, silt and clay that is periodically shifting due to physical and biological processes. The

vegetative cell must reach the surface via its own physical motion or be "mixed" upward. There is thus likely to be a critical depth below the sediment surface at which germinated cells are simply trapped in the sediment (over seasonal time scales) and never reach the water column. The depth of sediment that is mixed over monthly time scales offers a suitable first estimate for the depth scale. This depth can be approximated using short-lived natural radio-isotopes such as ^{234}Th or ^{7}Be, or artificially labeled sediment. Keafer et al. (1992) found ^{234}Th (half-life 24.1 days) was strongly depleted in the top 0.5-1 cm of sediment at station 29, which has sediment conditions typical of the large cyst-beds in the Gulf of Maine.

3.2 Function Construction

The approach to modeling the net effect of the complex processes above is to define a germination depth (d_g) chosen to represent the mean depth of sediment over which cysts are exposed to enough oxygen for germination and can reach the water column. The most direct estimates of this depth within the silt/clay sediments of the deeper regions of the Gulf of Maine comes from the combined results Anderson and Keafer (1985), Keafer et al. (1992), and Hines (1991), which suggest $d_g \sim 1$ cm. Results in Massachusetts Bay and in Long Island sound are not grossly inconsistent with this estimate (Aller and Cochran 1976; Benninger et al. 1979; Krishnaswami et al. 1980; Wheatcroft et al. 1994), although the reporting mixing depth is slightly larger. However, these results come from shallower water and, in the case of Massachusetts Bay, more sandy sediment than the conditions within the larger cyst beds.

It is assumed that mixing processes over the upper d_g centimeters maintains a relatively uniform cyst concentration, which allows approximation of the cyst flux without a z-dependence in the cyst concentration term.

The daylight-averaged irradiance is exponentially attenuated within the sediment:

$$E(z) = E_{bottom} \times e^{-k_s z}$$

Using k_s as estimated by Kuhl and Jorgensen. A central value of 3.5 mm^{-1} is chosen, and a range between 2 and 5 mm^{-1} is considered. E_{bottom} in the above expression is the irradiance at the bottom of the water column (i.e. the sediment surface).

3.3 Discussion

The primary assumptions of this approach are:

1. The cyst distribution over the top d_g centimeters is approximately uniform throughout the bloom season.
2. Spatial and temporal variation of d_g is secondary to the overall mean value.
3. The instantaneous germination rate of cysts is not heavily influenced by the time history of germination conditions over the time scales imposed by sediment mixing.
4. Re-supply of cysts from below d_g is negligible over the course of a bloom season (although not necessarily on inter-annual time scales).

Each of these assumptions are discussed below within the context of the Gulf of Maine. They should be revisited if applying this model to a different region.

Regarding assumption 1, observations of cyst variability within the top centimeter for the Gulf of Maine are very rare. One observation from station 29 (Anderson et al. unpublished data) shows 570 cysts/cm^3 from 0-0.5 cm, and 651 cysts/cm^3 from 0.5-1 cm which, given the observed variability in cyst concentration over several orders of magnitude within the Gulf of Maine, supports the assumption of uniformity. In addition, the fact that d_g was chosen to represent the depth of the rapidly mixed zone is consistent with this assumption.

Mixing rates below this upper layer quickly fall to 1-3% the mixing rate within it (Krishnaswami et al., 1980), suggesting that the upward flux of cysts from below the rapidly mixed layer is minimal during the bloom season. However, it is notable that this could be circumvented by persistent transport from deeper areas resulting from complex feeding behavior of benthic fauna.

Spatial variability in d_g is likely to result from gradients in benthic fauna and flora, changes in sediment type, changes in the energy of the overlying flows, and gradients in the amount of organic matter arriving at the sediment. The majority of cysts observed in the Gulf of Maine lie in similar sediments in relatively deep water (i.e. > 75 meters). This would tend to minimize spatial variability in d_g and support a spatially uniform d_g as a good starting point.

Temporal variability in sediment mixing rates has been noted in the aforementioned studies by Aller et al. (1976) and Wheatcroft et al. (1994). In both cases, the trends were attributed to seasonal shifts abundance and activity of benthic fauna. Mixing rates showed a distinct Fall maximum. Present simulations focus on the spring and summer time period, over which little and the value of d_g is chosen to reflect mixing

during this time. Thus, although temporal variability in d_g may be significant for inter-annual simulations, it can probably be neglected in the present simulations, which primarily cover only the spring and summer.

Within the Gulf of Maine, simulations were highly influenced by uncertainty in d_g (Stock et al., 2005). A range of d_g from 0.5-1.5 cm was considered, essentially amounting to a factor of three uncertainty in the overall size of the source. Increased knowledge of sediment dynamics and their effect on the germination source would cut down this uncertainty, and provide for a more useful modeling tool.

Aller, R. C. and J. K. Cochran (1976). $^{234}T/^{238}U$ disequilibrium in nearshore sediment: particle reworking and diagenetic time scales. Earth and Planetary Science Letters **29**: 37-50.

Anderson, D. M. (1998). Physiology and bloom dynamics of toxic *Alexandrium* species, with emphasis on life cycle transitions. Physiological Ecology of Harmful Algal Blooms. D. M. Anderson, A. D. Cembella and G. M. Hallegraeff. Berlin, Springer-Verlag. **G 41:** 29-48.

Anderson, D. M., D. G. Aubrey, M. A. Tyler and W. D. Coats (1982). Vertical and horizontal distributions of dinoflagellate cysts in sediments. Limnology and Oceanography **27**(4): 757-765.

Anderson, D. M. and B. A. Keafer (1985). Dinoflagellate cyst dynamics in coastal and estuarine waters. Toxic Dinoflagellates: Proceedings from the third International Conference. D. M. Anderson, D. G. Baden and A. W. White. Amsterdam, Elsevier**:** 219-224.

Anderson, D. M. and B. A. Keafer (1987). The endogenous annual clock in the toxic dinoflagellate Alexandrium tamarensis. Nature **325**(6105): 616-617.

Anderson, D. M., C. A. Stock, B. A. Keafer, A. B. Nelson, B. Thompson, D. J. McGillicuddy, M. Keller, P. A. Matrai and J. Martin (2005). Alexandrium fundyense cyst dynamics in the Gulf of Maine. Deep-Sea Research Part II-Topical Studies in Oceanography **52**(19-21): 2522-2542.

Anderson, D. M., C. D. Taylor and V. E. Armbrust (1987). The effects of darkness and anaerobiosis on dinoflagellate cyst germination. Limnology and Oceanography **32**(2): 340-351.

Benninger, L. K., R. C. Aller, J. K. Cochran and K. K. Turkekian (1979). Effects of biological sediment mixing on the ^{210}Pb chronology and trace metal distribution in a Long Island Sound sediment core. Earth and Planetary Science Letters **43**: 241-259.

Bewley, J. D. and M. Black (1978). Physiology and biochemistry of seeds in relation to germination. New York, Springer-Verlag.

Bronzino, A. C. (1998). *Alexandrium* spp. cyst dynamics and their significance in bloom initiation in the Gulf of Maine. Woods Hole, MA, Woods Hole Oceanographic Institution.

Keafer, B. A., K. O. Buesseler and D. M. Anderson (1992). Burial of living dinoflagellate cysts in estuarine and nearshore sediments. Marine Micropaleontology **20**: 147-161.

Krishnaswami, S., L. K. Benninger, R. C. Aller and K. L. Von Damm (1980). Atmospherically-derived radio-nuclides as tracers of sediment mixing and accumulation in nearshore marine and lake sediments: evidence from ^{7}Be, ^{210}Pb, and $^{239,240}Pu$. Earth and Planetary Science Letters **47**: 307-318.

Kuhl, M. and B. B. Jorgensen (1994). The light of microbenthic communities: Radiance distribution and microscale optics of sandy coastal sediments. Limnology and Oceanography **39**(6): 1368-1398.

Matrai, P., B. Thompson and M. D. Keller (2005). Circuannual excystment of resting cysts of *Alexandrium* spp. from eastern Gulf of Maine populations. Deep Sea Research Part II **52**: 2560-2568.

McGillicuddy, D. J., D. M. Anderson, D. R. Lynch and D. W. Townsend (2005). Mechanisms regulating large-scale seasonal fluctuations in Alexandrium fundyense populations in the Gulf of Maine: Results from a physical-biological model. Deep-Sea Research Part II-Topical Studies in Oceanography **52**(19-21): 2698-2714.

Mcgillicuddy, D. J., R. P. Signell, C. A. Stock, B. A. Keafer, M. D. Keller, R. D. Hetland and D. M. Anderson (2003). A mechanism for offshore initiation of harmful algal blooms in the coastal Gulf of Maine. Journal of Plankton Research **25**(9): 1131-1138.

Stock, C. A., D. J. McGillicuddy, A. R. Solow and D. M. Anderson (2005). Evaluating hypotheses for the initiation and development of Alexandrium fundyense blooms in the western Gulf of Maine using a coupled physical-biological model. Deep-Sea Research Part II-Topical Studies in Oceanography **52**(19-21): 2715-2744.

Sweeney, B. M. (1969). Rhythmic phenomena in plants. New York, Academic Press.

Wheatcroft, R. A., I. Olmez and F. X. Pink (1994). Particle bioturbation in Massachusetts Bay: Preliminary results using a new deliberate tracer technique. Journal of Marine Research **52**: 1129-1150.

Table 1: Fitted slopes and 90% confidence intervals for each germination time series.

Temperature (^{o}C)	Dark Rate (WGOM)	Dark Rate (EGOM)	Light Rate (WGOM)	Light Rate (EGOM)
2	0.91 (0.25)	1.21 (0.34)	0.89 (0.27)	1.74 (0.62)
4	0.82 (0.24)	1.43 (0.30)	1.69 (0.22)	1.74 (0.77)
6	1.19 (0.17)	1.70 (0.37)	2.03 (0.52)	1.58 (0.34)
8	1.40 (0.32)	3.32 (0.60)	6.55 (1.76)	4.03 (0.60)
15	NA	4.24 (0.48)	NA	8.72 (3.51)

Table 2: Parameters fit to the germination function

parameter	units	$E = E_{lgt}$	$E = E_{drk}$
α	$(^{o}C)^{-1}$	0.790	0.394
β	dimensionless	6.27	3.33
G_{max}	%/day	8.72	4.26
G_{min}	%/day	1.50	1.04

Table 3: Data sets used for the construction of the endogenous clock.

Station # (see fig. 1)	Reference	Latitude (N)	Longitude (W)	Depth	Date of Isolation
29 (1)	Anderson and Keafer (1987)*	43	70.19’	146	Aug. 1984
29 (2)	Anderson and Keafer (1987)*	43	70.19’	146	July 1985
29 (3)	Anderson and Keafer (1987)*	43	70.19’	146	June 1986
38	Bronzino (1998) Anderson et al. (2005)	43^{o} 30.29’	69^{o} 52.72’	125	late Jan. early Feb. 1999
61	Matrai et al. (2005)	43^{o} 34’	69^{o} 27’	150	Dec. 9 1999
94	Matrai et al. (2005)	43^{o} 40’	68^{o} 38’	150	Dec. 10 1999
4	Matrai et al. (2005)	44^{o} 53.5’	66^{o} 49’	138	Jan. 27 2000

* Only a portion of the data from the August 1984 station was presented in the reference. Time series were continued after publication and on multiple isolates to verify the clock.

Table 4: Monthly values of the germination potential (GP, %), and the normalized germination potential (NGP)

	Jan	Feb	Mar	Apr	May	June	July	Aug	Sep	Oct	Nov	Dec
GP	21.9	11.25	78.0	85.0	96.8	93.0	60.0	50.0	10.0	11.5	17.0	25.0
NGP	0.23	0.12	0.81	0.88	1.00	0.96	0.62	0.52	0.10	0.12	0.18	0.26

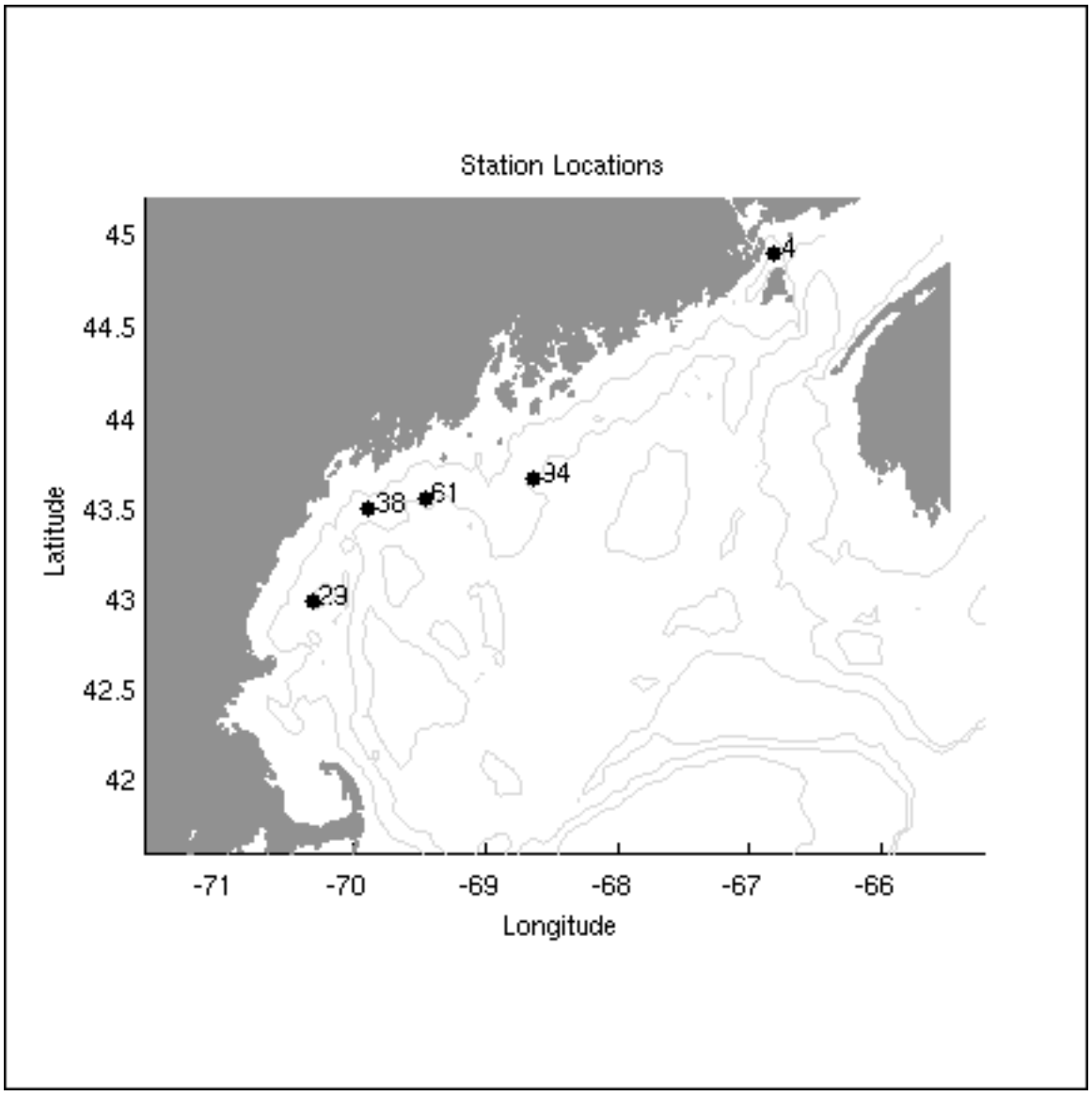

Figure 1: Stations where cysts were isolated for germination and endogenous clock experiments.

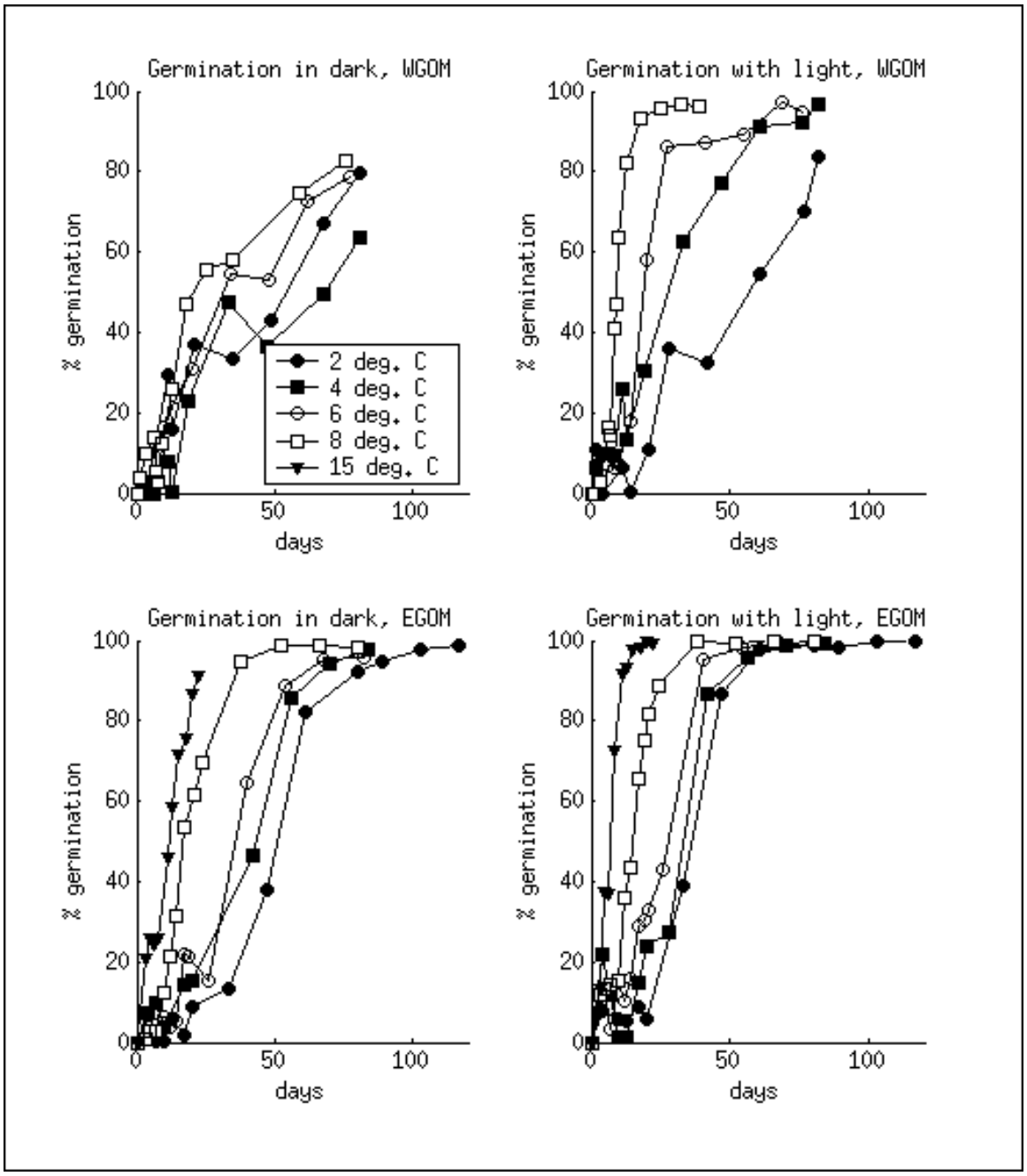

Figure 2: Germination time series data from station 38 (top panel, WGOM = Western Gulf of Maine), and data from station 4 (bottom panel, EGOM = Eastern Gulf of Maine). Note that a germination time series at 15^{o} C was not taken for the WGOM case.

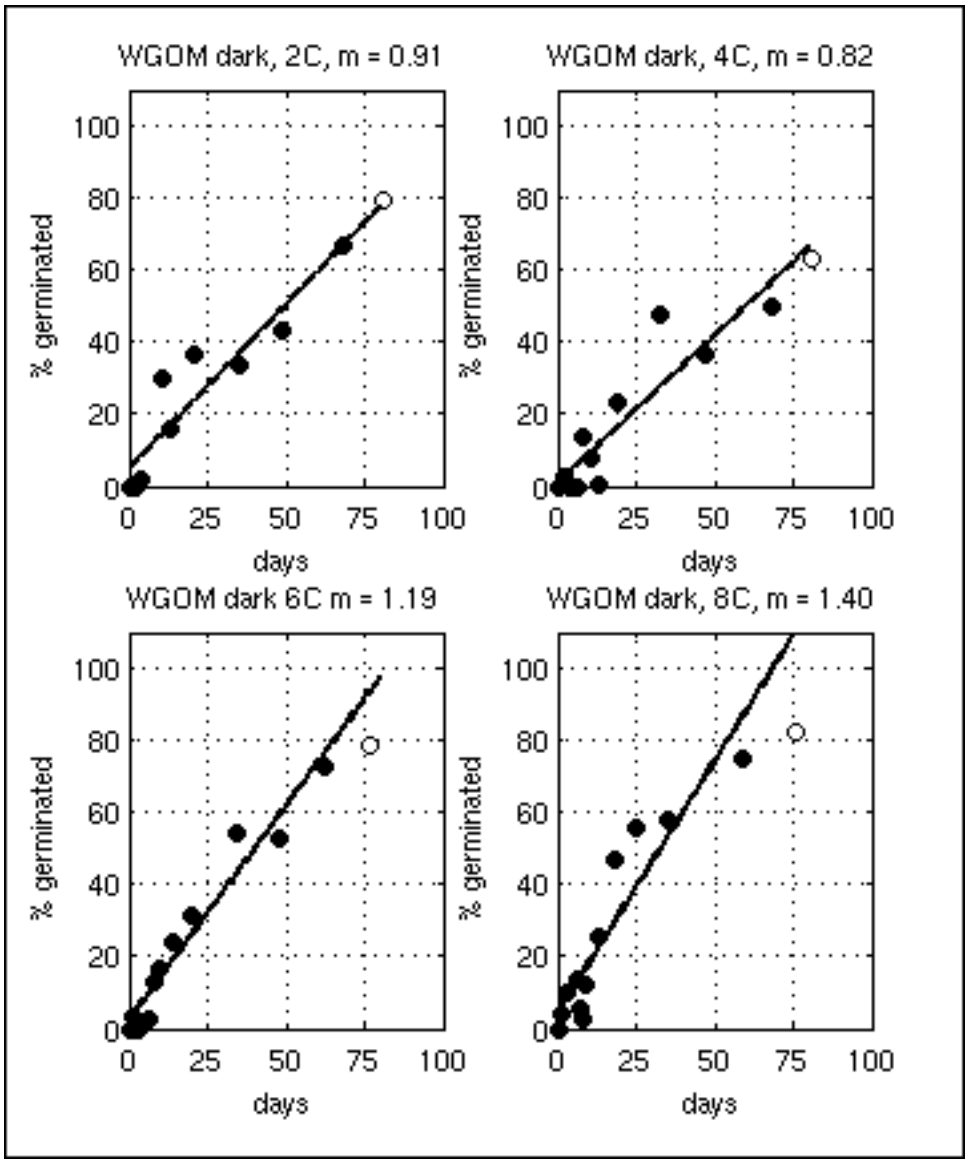

Figure 3: Fits to the WGOM (station 38) data in dark conditions. Solid circles are used in the fit, open circles are not.

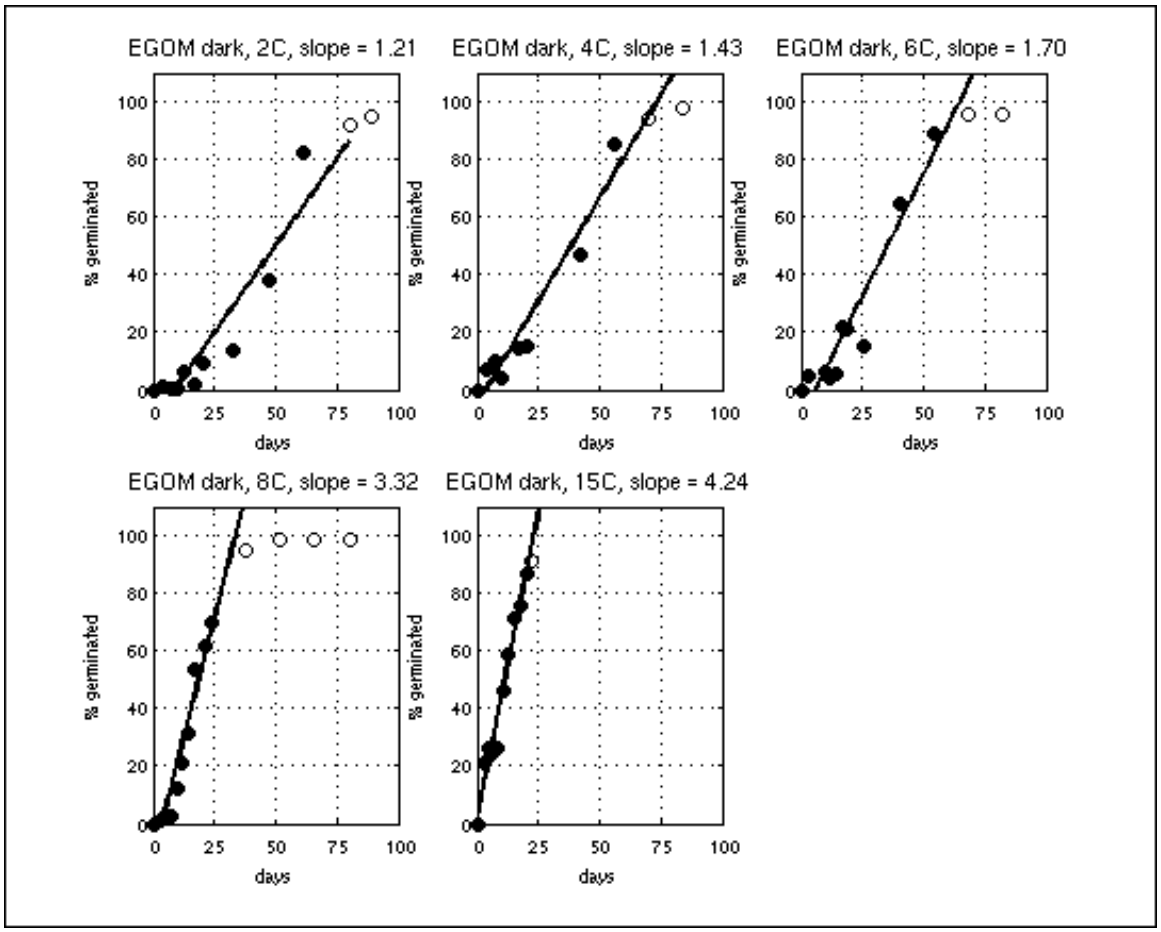

Figure 4: Fits to the EGOM (station 4) data with dark conditions. Solid circles are used in the fit, open circles are not.

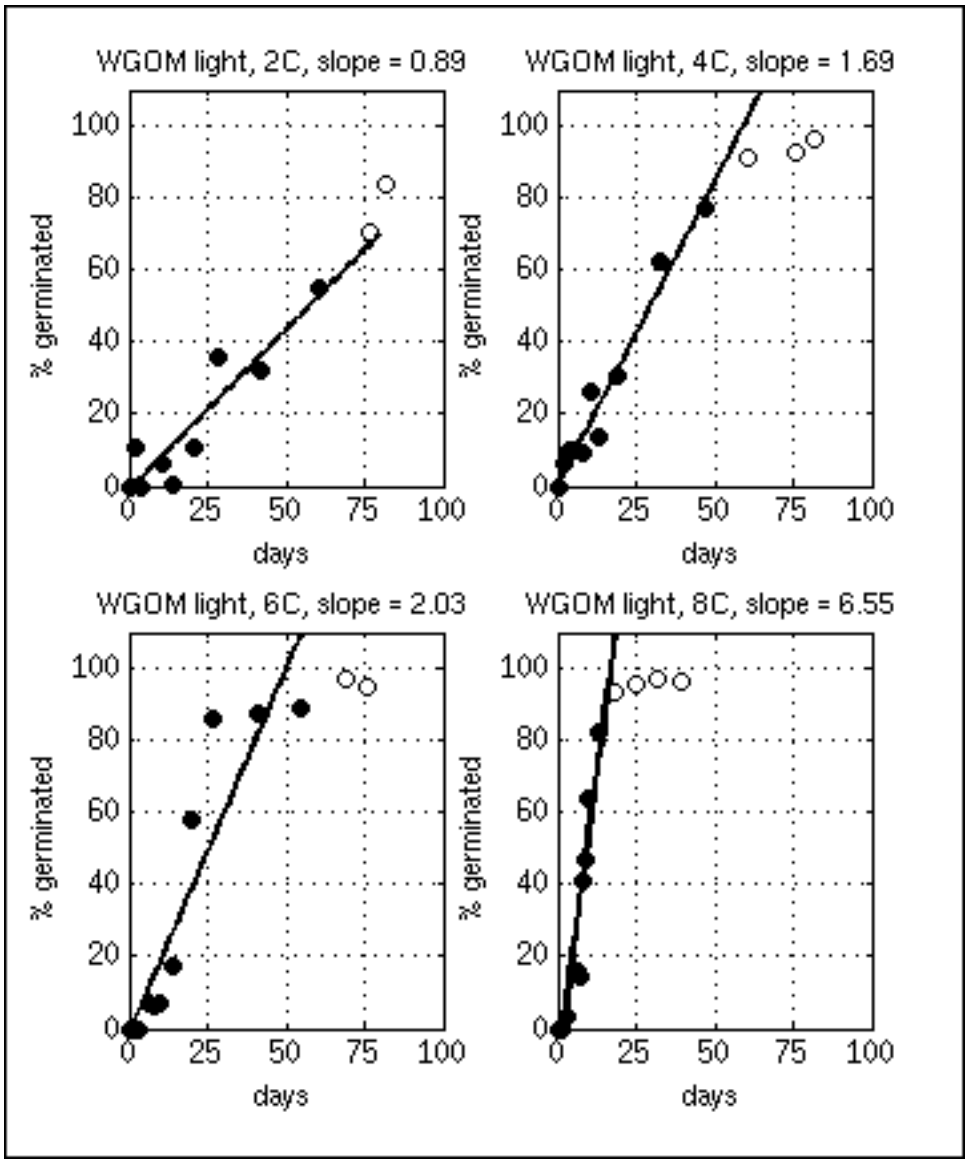

Figure 5: Fits to the WGOM (station 38) data with light conditions. Solid circles are used in the fit, open circles are not.

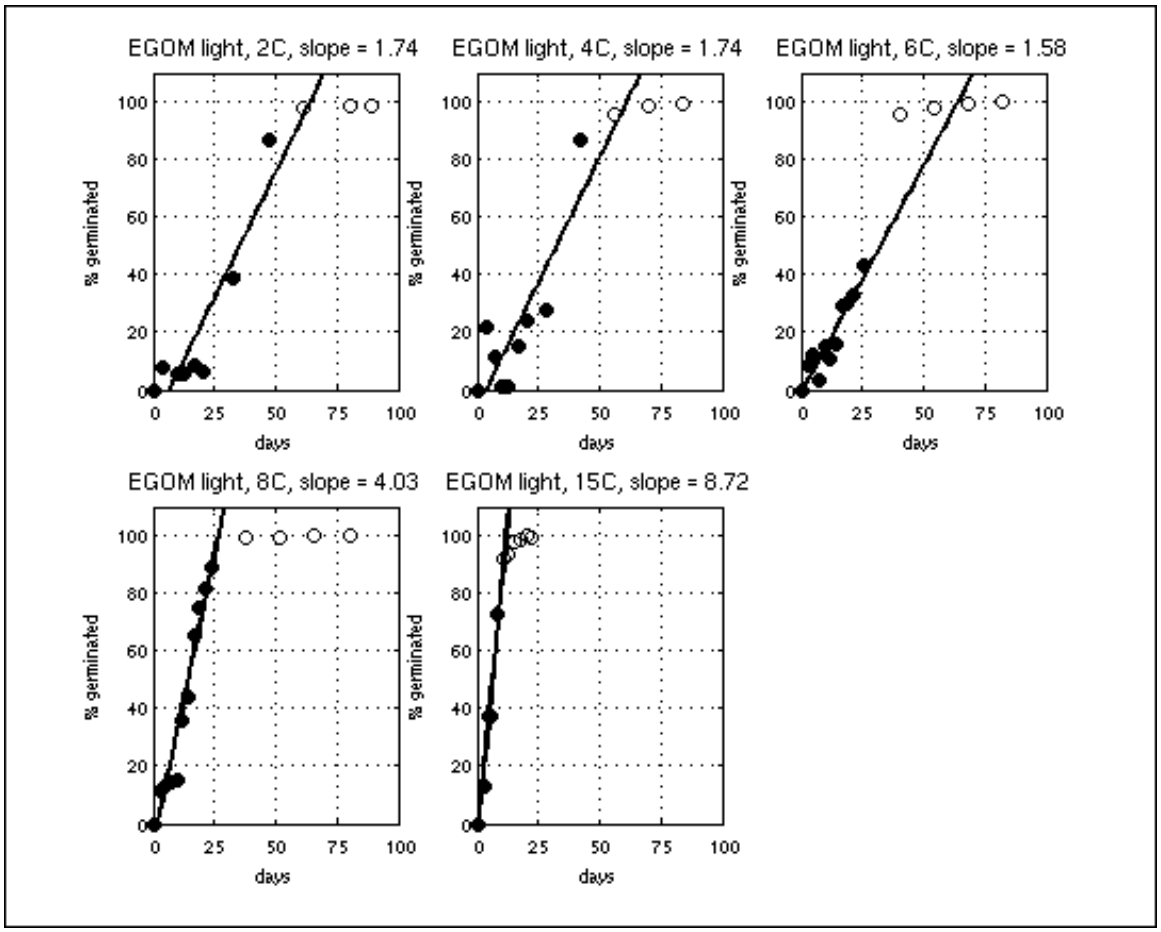

Figure 6: Fits to the EGOM (station 4) data with light conditions using the criteria described in section II above. Solid circles are used in the fit, open circles are not.

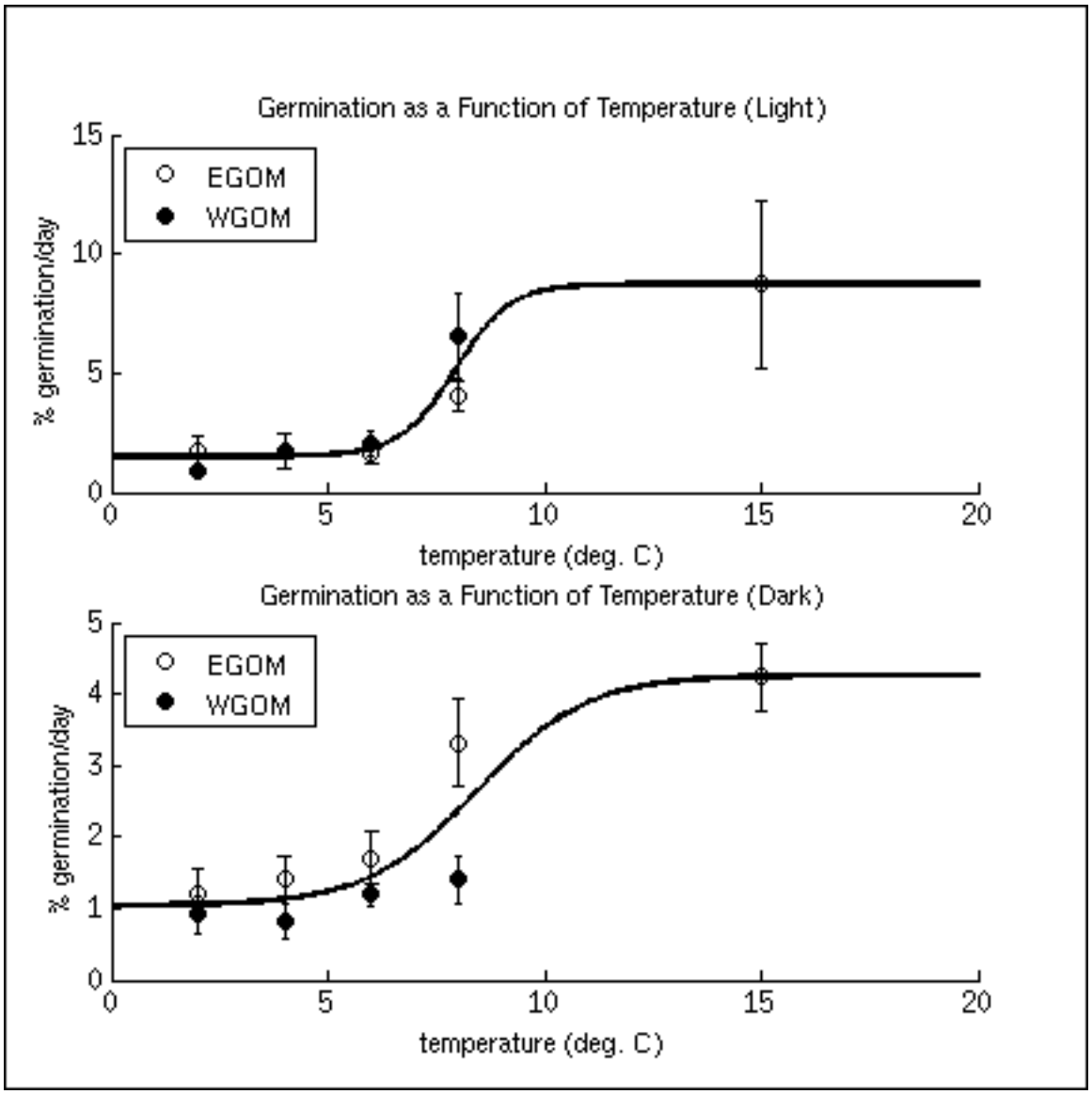

Figure 7. Germination as a function of temperature at $E=E_{lgt}$ (top panel) and $E=E_{drk}$ (bottom panel). The markers are experimental time series rate estimates with 90% uncertainty bounds (table 1). The dark line is the functional fit which drives the germination model. Parameters describing the fit are given in table 2. Note that the light rates a 4^{o}C in the EGOM and WGOM overlap closely, making the EGOM point difficult to detect.

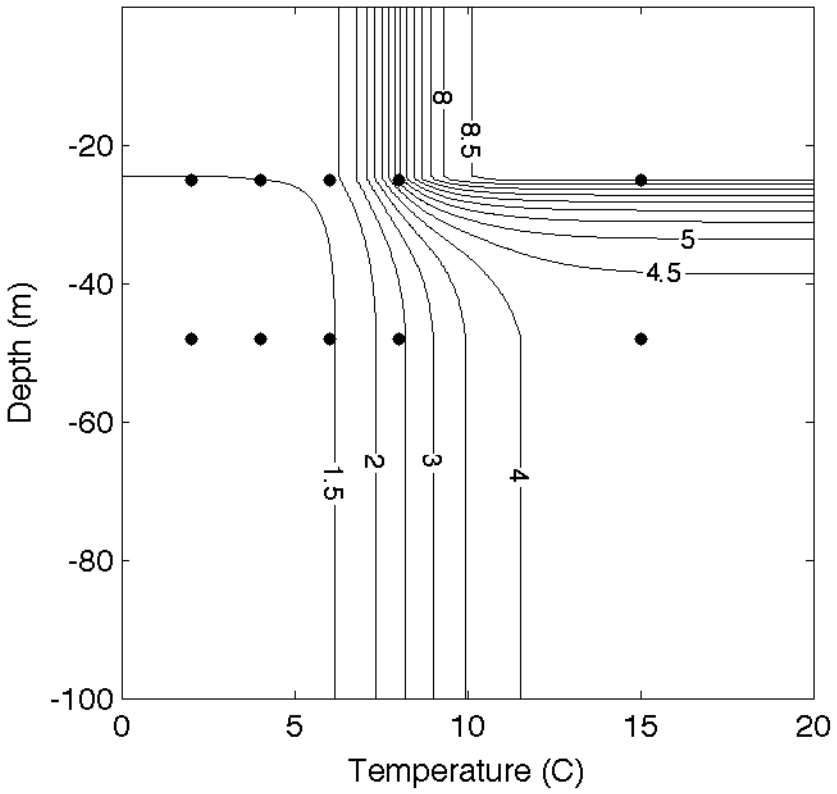

Figure 8: Contours (interval = 0.5 %/day)) of the model estimated germination rate (%/day) at the sediment surface as a function of light and temperature ($G(T,E)$). Light has been transformed to an equivalent depth using an exponential attenuation coefficient k_w = 0.2 m^{-1} and a typical day-averaged (8 AM-6 PM) irradiance of 345 watts/m^2. Markers show temperatures where experiments were carried out for light conditions (upper row) and dark conditions (bottom row). These estimates are at the sediment surface, and there is additional light attenuation over the top cm of the sediment (k_s = 3.5 mm^{-1}). **Note:** in Fig. 7 in Anderson *et al.* (2005), a point is shown at 5° C in the dark condition. This was from an earlier formulation and should have been omitted.

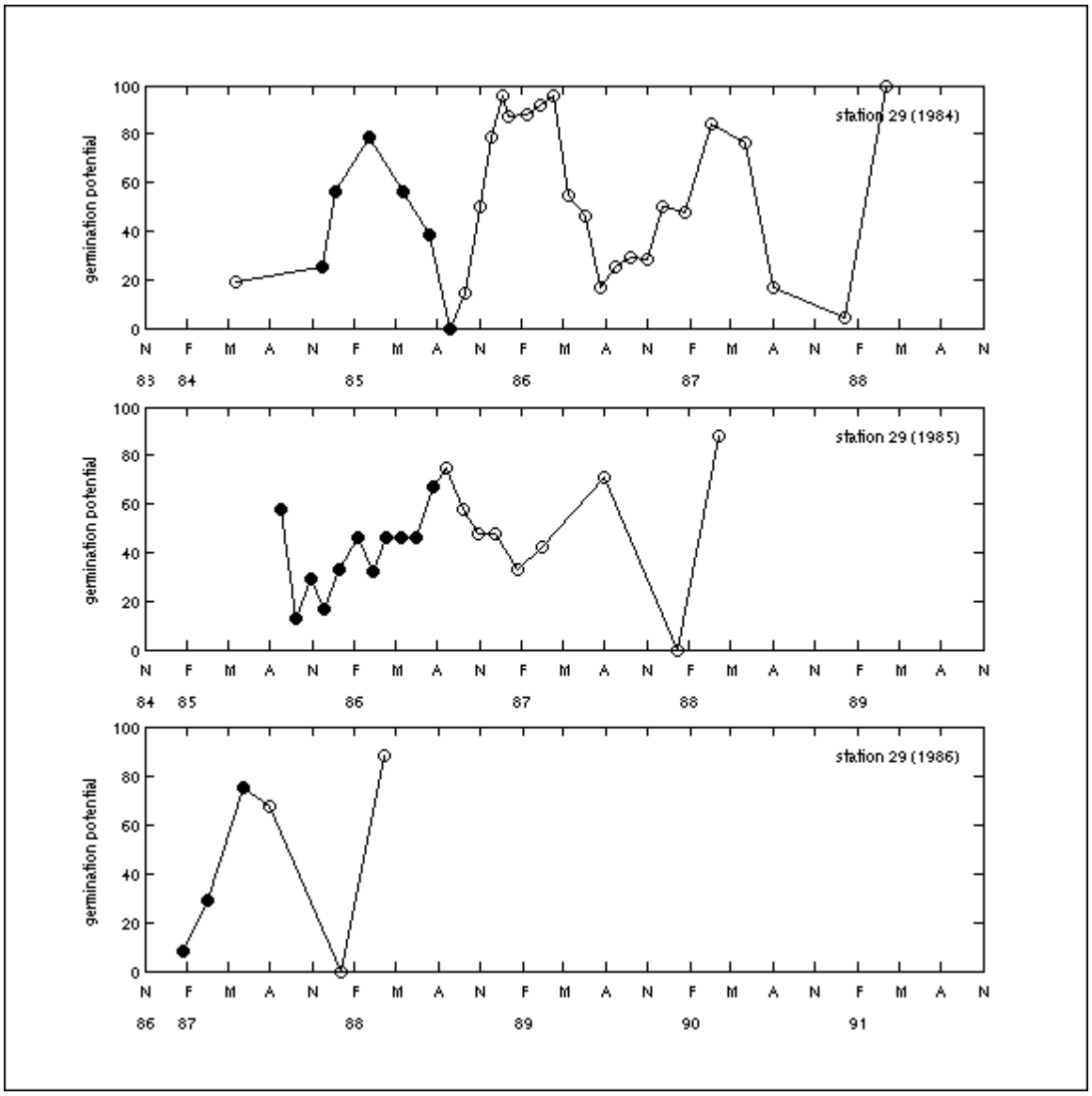

Figure 9: Endogenous clock experiment data for the three sediment isolations taken from station 29 near Cape Ann. Note that the axes are each 5 years in duration and all begin on November 1 to facilitate comparison of the shapes and phases of the germination potential data. “M” is May, "A" is August. Dates where experiments to measure the germination potential were *started* are shown as circles. Closed circles indicate points used in the formulation of the endogenous clock applied to the model, open circles are not. Note the early initial peak for the 1984 isolate (top panel) contrasted with the later peaks observed in 1985 and 1986. Also, note gradual climb to peak germination exhibited by the 1985 isolation. *Note that the first point in the 1984 time series is from an earlier sediment isolation at the same location, and it is thus not used in the model. Also, the 1986-87 experiment was carried out with an isolate initially taken in June of 1986 and experiments weren’t started until later in the year.*

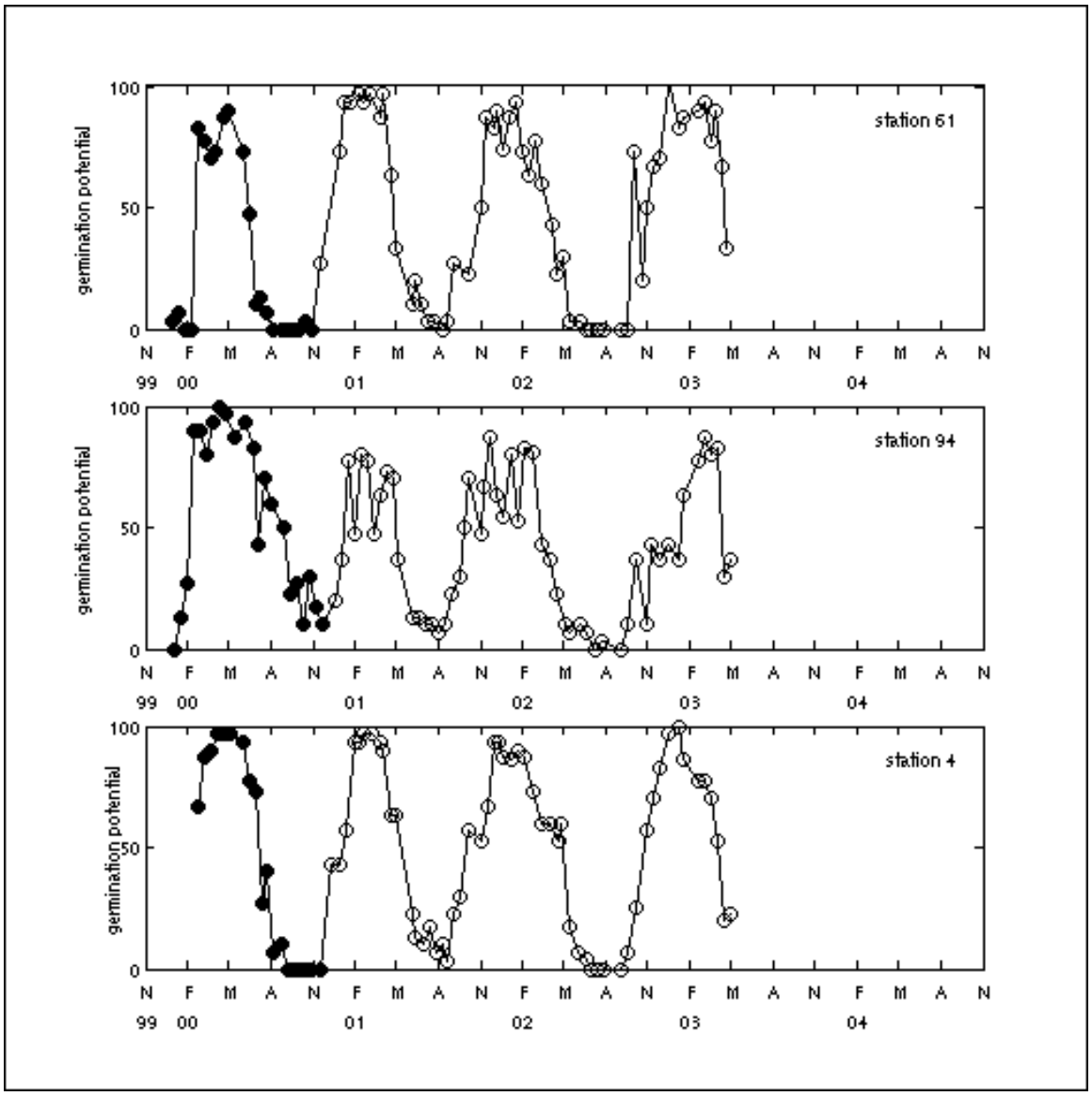

Figure 10: Endogenous clock experiment data for the three isolates presented in Matrai et al. (2005). Notation is as in Figure 9. Note the fairly consistent late winter, early spring initial peak that is generally maintained into the early summer, also note the gradual decline in germination potential exhibited by station 94.

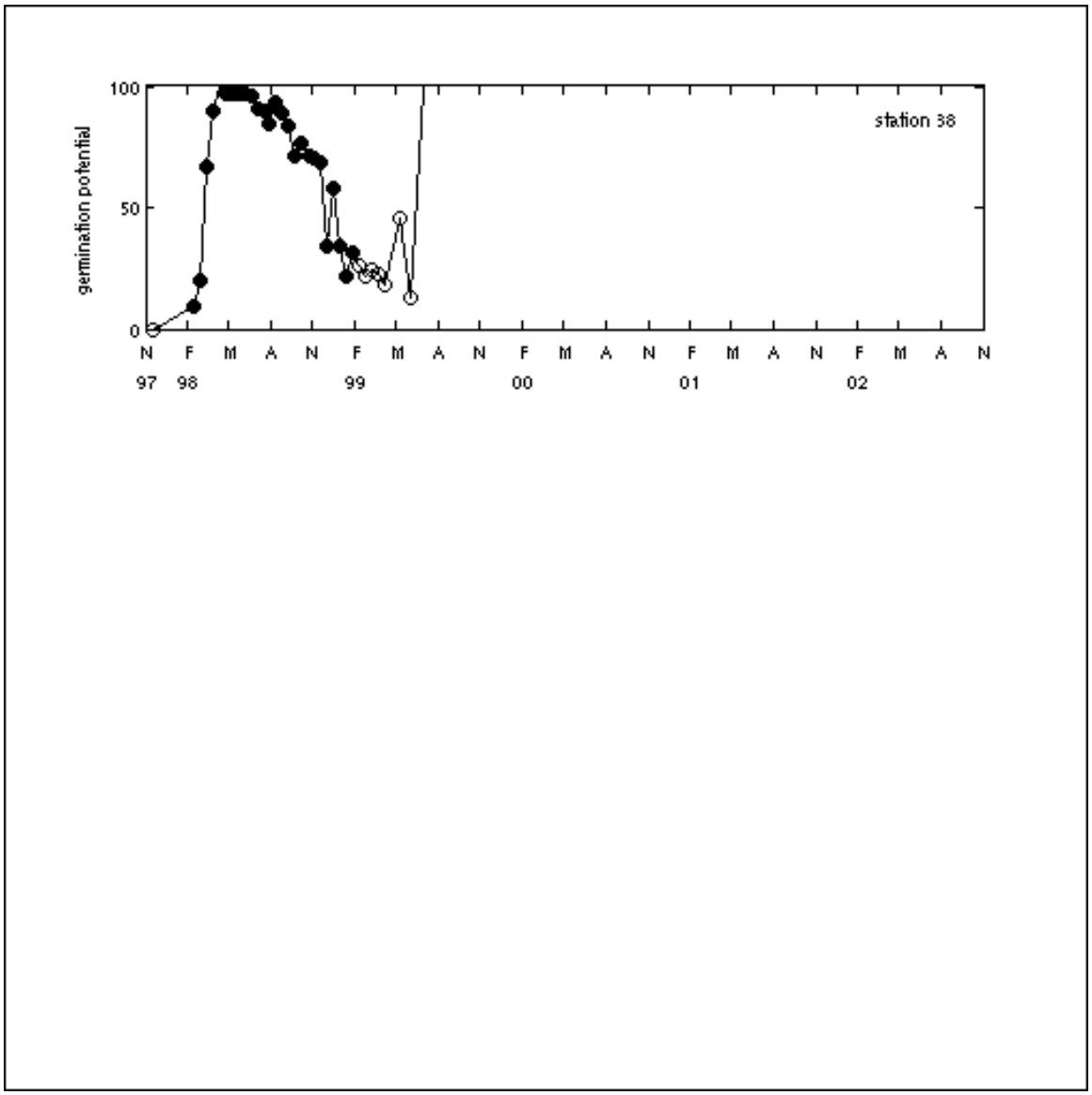

Figure 11: Endogenous clock data presented in Bronzino (1998). Notation is as in figures 9 and 10. The initial peak is in late March/early May, and the decline in germination potential after the peak is very slow. *Note that the first point in the data set is the result of an earlier isolation of cysts at the same location and it is thus not included in the model.*

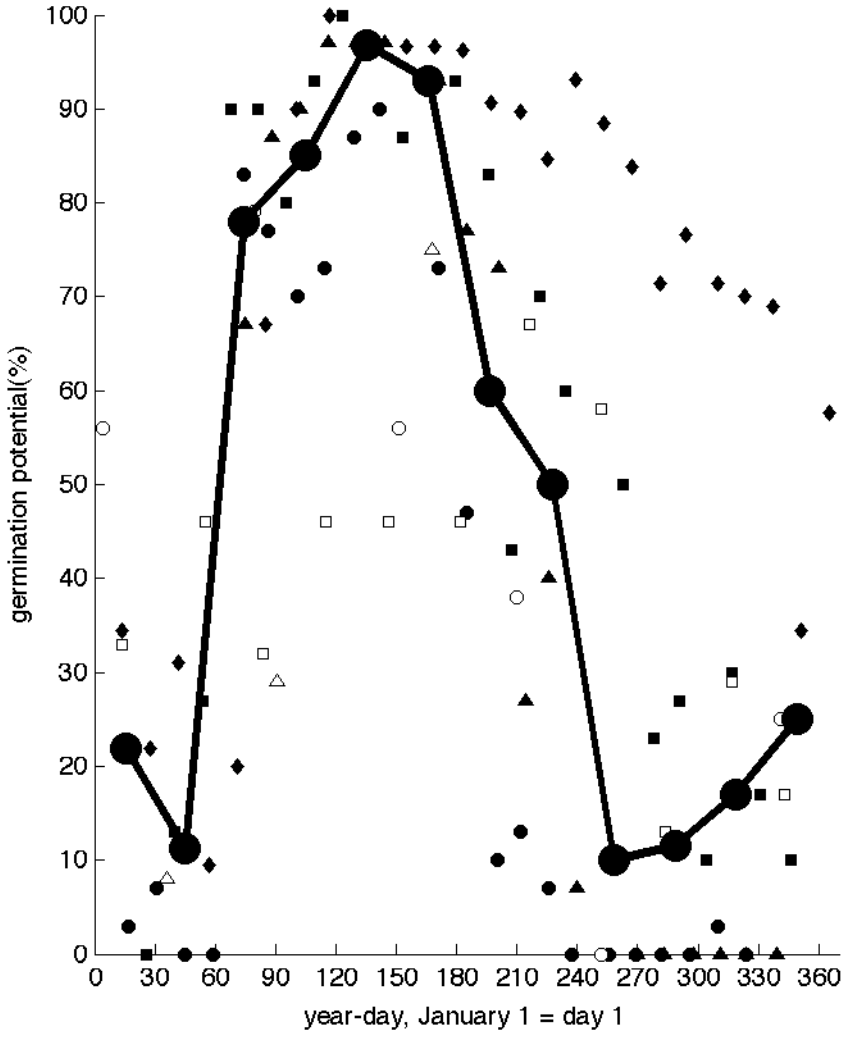

Figure 12: Data used for the specification of the endogenous clock (see legend) and resulting germination potential function (dark line). Large filled squares mark the mid-points of the months where the germination potential was estimated. **Note:** The value of the December point was shown as 34.5 in Anderson et al. (2005). This is has been corrected to a value of 25.0.